EE 495 PROJECT REPORT

Optimization of a Polarized Muon Beam

Lance Doherty
ID: 243341

April 14, 1998

Supervisor: Dr. N. Rodning
Department of Physics

Abstract

This report outlines the successful design and computer simulation of a spin-polarized positive muon beamline. The muon beam selected by the system is a component of TRIUMF E614, an experiment to measure the Michel spectrum of polarized muon decay. The experiment requires an accurately polarized beam of muons to obtain a precise characterization of the decay. Detection of the decay occurs midway through a 2m long, 2T solenoid. The beam optical transformation of a half-solenoid is derived and implemented in the simulation software. The chosen beamline design provides a muon beam with 13.9mRad composite divergence with no scattered particles reaching the target. With one million particles emitted from the source, 1,560 reach the target. Error boundaries on the initial beam conditions and the solenoidal fields are calculated. Confirmation of the effectiveness of spatial filtering is also examined. Limited by memory requirements, quantitative confirmation of the scattering requirement was not obtained.

Acknowledgment

I would like to thank Dr. Nathan Rodning for his contributions to this project. In addition to providing me with a set of realistic goals, he put aside time every week to answer my many questions. My work under his supervision in the past two years has given me a great appreciation for experimental physics. If I were staying at the U of A for my graduate work….

BACKGROUND **1**
THE STANDARD MODEL AND MUON DECAY 1
GENERATING AND TRANSPORTING MUONS 1
OBJECTIVES **2**
THEORY **3**
DEFINITION OF TERMS 3
HALF-SOLENOID TRANSFER MATRIX 4
STATISTICAL APPROACH 5
LIOUVILLE'S THEOREM 5
EXPERIMENTAL METHOD **6**
BEAMLINE SIMULATION 6
Intran – running the TRANSPORT algorithm *6*
Revmoc – tracking individual particles *6*
EXPERIMENTAL FILTERING 7
BEAMLINE DESIGN 8
SOLENOID FACING 9
RESULTS AND ANALYSIS **10**
THE THREE-VARIABLE BEAMLINE 10
THE SINGLE-VARIABLE BEAMLINE 11
SCATTERING IN THE BEAMLINE 13
SENSITIVITY TO INITIAL BEAM PARAMETERS 15
SENSITIVITY TO SOLENOIDAL FIELD 15
FINAL DRIFT REGION DISTANCE 16
CONCLUSIONS **18**
REFERENCES **19**
APPENDIX A – SAMPLE INTRAN INPUT FILE **20**
APPENDIX B – SAMPLE REVMOC INPUT FILE **21**
APPENDIX C – SAMPLE REVMOC OUTPUT **22**
APPENDIX D – SAMPLE PAW MACRO FILE **23**

Background

The Standard Model and Muon Decay

The theoretical behaviour of elementary particles is collected in what is known as the "Standard Model". This model explains the strong, weak, and electromagnetic interactions in nature. Furthermore, no experiment has yet found a flaw in the model. Experiments seeking to test the validity of the Standard Model fall into three categories:

1. high-energy experiments searching for new phenomena and more massive particles
2. searching for processes forbidden by the Standard Model
3. high precision measurements of processes well-defined by the Standard Model

The goal of any of these experiments is to find fault with the Standard Model, and gain deeper insight into particle interactions with the development of new physics. More likely, however, the experiment will agree with the Standard Model, increasing the precision to which we understand the universe. TRIUMF E614 is an experiment belonging to the third category of tests.

TRIUMF E614 will measure the Michel spectrum from spin-polarized muon decay. This spectrum is characterized by four independent parameters, which can be determined with a precise mapping of the spectrum. These four parameters are intrinsic to the weak interaction, and have precisely predicted values in the Standard Model. TRIUMF E614 seeks to determine these parameters to higher precision than previously measured. It is essential to the experiment that a highly spin-polarized beam of muons can be trapped for decay. Any errors in the spin-polarization of the muons reduce the precision of the measured Michel parameters.

Generating and Transporting Muons

The primary goal of this project is to design a spin-polarized muon beam to be used in TRIUMF E614. An existing setup is used to generate the positively charged muons. A beam of protons is fired at a fixed metal target. Pions created in the proton-target collision decay within the target, producing muons which have their spin oriented opposite to their momentum. The spin-polarization is ensured by the conservation of linear and angular momentum in a two-body interaction. Collisions between muons and other particles inside the target reduce the momentum of the muons and randomize their spin. Since spin-polarization must be maintained, it is preferable to select muons produced near the surface of the target where they have the least chance of a spin-randomizing collision. This can be done by selecting the highest muon momentum – muons produced deeper in the target will have less momentum and will not be selected by the system.

Selection of muon momentum is accomplished by charged particle beam optics. Analogous to light optics, this technique uses magnets and slits to mimic lenses and apertures. The muon beam is directed to a new target that stops the selected muons and holds them until decay. The positrons produced in the decay allow for the measurement of the Michel spectrum. This project seeks to optimize the mechanism used to guide the muons from source to target along the beam line.

Objectives

The precise nature of the decay measurements requires that the polarization of a decaying muon must be defined to high accuracy. This requirement is defined by the following three criteria:

1. the direction of propagation and spin-polarization are coupled; angular deviations of the beam must be less than 14.1 milliradians to indirectly control the polarization
2. the probability of an individual muon in the beam being scattered must be less than 10^{-4} – this limits uncertainty in polarization directly
3. the number of muons reaching the target must be sufficiently large to accumulate 10^9 decay events in approximately two weeks – this project is concerned only with obtaining the highest number of muons from the source reaching the target

A correct "tuning" of the magnetic guidance channel can achieve these three criteria.

A representative sketch of the magnetic channel is illustrated in the figure below. Desired muons will follow the solid line, the "beamline", through the system. Triangular elements are dipole (bending) magnets, used to curve the muon beam. Together with the slits that pass only a portion of the beam, unwanted particles (i.e. muons with incorrect momenta and particles other than muons) are removed from the system. The overall effect of the system is to allow only muons with the required properties to reach the target where the decay will be observed. The quadrupole (focusing) magnets, shown as concave and convex lenses, serve to focus the particle beam to reduce the angular variation in the beam at the target. Adjustment of the quadrupole strengths, like lenses in an optical system, tunes the sharpness of the beam image at the target.

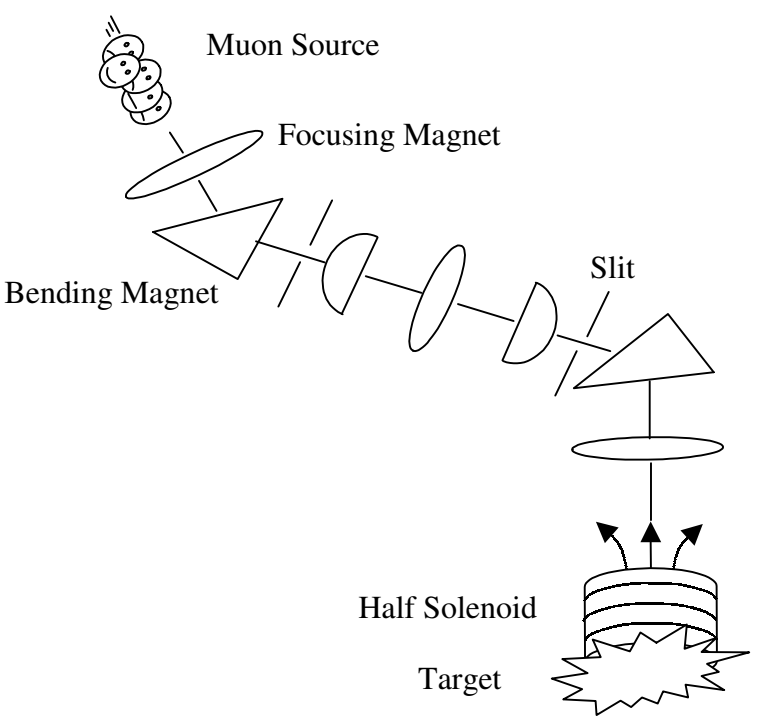

Optimization of the magnetic channel is done through computer simulation. The simulations provide a near-analytical solution. As such, simulation in this sense is akin to an actual physical testing of the system.

In addition to the magnets providing the particle beam optics, a large solenoid is used in the system as part of the detection mechanism. The target is located midway through the solenoid – an effective "half-solenoid" transfer matrix is derived as part of this project. Finding a suitable position for the solenoid is central to the beamline optimization. An incorrect positioning of the solenoid introduces intolerable errors into the Michel parameter measurement.

Theory

Definition of Terms

Using beam optics, a mathematical model of the muon beam system can be described. First, consider that a particle can be characterized by a 4-parameters in a vector space. Furthermore, this vector representation is time dependent – or, as is the convention in beam optics, this vector is a function of the location on the beamline. This beamline distance coordinate is labeled as "z", starting from zero at the source. For z > 0, a local Cartesian coordinate frame is defined with the z unit vector pointing "downstream" from the source. This is the average direction of propagation of the muons from this point. At a given z, a muon is represented by:

- x : Distance Perpendicular to the beamline in x-direction [cm]
- dx/dz (or just dx) : Deviation from the beamline in x-direction [mRad]
- y : Distance Perpendicular to the beamline in y-direction [cm]
- dy: Deviation from the beamline in y-direction [mRad]

Other beam parameters (such as divergence) are not relevant to this analysis and are hence omitted. The composite divergence is obtained by adding dx and dy in quadrature.

Transformations in this vector space are carried out using 4x4 matrices. The meaning of each entry in a matrix is intuitive – for example, the (1,2) element specifies how much of the initial dx is mixed into the final x. The application of several transformations is evaluated using matrix multiplication. Hence, the final beam characteristics of an "n" element system can be generated from the initial beam characteristics as follows:

$$\begin{bmatrix} final \\ beam \\ characteristics \end{bmatrix} = \begin{bmatrix} Transfer \\ Matrix \\ n \end{bmatrix} \begin{bmatrix} Transfer \\ Matrix \\ n-1 \end{bmatrix} \cdots \begin{bmatrix} Transfer \\ Matrix \\ 1 \end{bmatrix} \begin{bmatrix} initial \\ beam \\ characteristics \end{bmatrix}$$

The aggregate transfer matrix describing the optical effect of the beamline will be called "R". Individual elements of R are indicated by the row and column of the entry – for example, R12 is the (1,2) entry of R. Physically, beam transformations are the result of magnetic fields. Classes of magnetic fields have well documented (see [1] for example) transfer matrices, as does a field-free, or drift, region. The transfer matrix of a solenoid can be referenced - the corresponding half-solenoid matrix derivation is part of this project.

Half-Solenoid Transfer Matrix

The effect of an entire solenoid is beam optically characterized by two parameters, the length "L" and the central field "Bz". The derivation of this transformation is broken up into three segments: exit matrix, centre matrix, entry matrix. In this project, the target is located midway through the solenoid – hence a transformation representing the entry and ½ of the centre matrix is required. A slightly flawed derivation of the entry field matrix can be found in [5]. By following the same physics, the entry field is:

$$T_{entry} = \begin{bmatrix} 1 & 0 & 0 & 0 \\ 0 & 1 & \frac{\theta}{2L} & 0 \\ 0 & 0 & 1 & 0 \\ -\frac{\theta}{2L} & 0 & 0 & 1 \end{bmatrix} \quad \text{э}\,\theta = \frac{B_z L}{(B\rho)_o}$$

The denominator of theta is a function of the incoming particle's momentum at the entrance to the solenoid. Theta varies linearly with both the central field strength and the solenoid length. This simple expression follows from two assumptions:

- the fringe field is short – all field lines curve back to the other end of the solenoid in a distance much less than that to the previous magnetic element
- the radial component of the entry field is linear with the perpendicular distance from the beam axis – this is a first-order approximation

The exit matrix is the same as the entry matrix, save for the off-diagonal elements being replaced by their additive inverses. Later, when error boundaries are discussed, scaling of the fringe field relates to multiplying the off-diagonal elements of the entry matrix above.

The interior field is aligned along the beam axis as in an ideal solenoid. Again, the derivation is presented (with another small error) in [5]. The central field is characterized by:

$$T_{centre} = \begin{bmatrix} 1 & \frac{L}{\theta}\sin\theta & 0 & \frac{L}{\theta}(1-\cos\theta) \\ 0 & \cos\theta & 0 & \sin\theta \\ 0 & \frac{L}{\theta}(\cos\theta - 1) & 1 & \frac{L}{\theta}\sin\theta \\ 0 & -\sin\theta & 0 & \cos\theta \end{bmatrix}$$

Theta is the same as for the entry matrix. To represent half of central region, the "square root" of this matrix is taken. Not surprisingly, this is equivalent to the transformation L→½L. Since theta is a function of L, theta changes for the central matrix (but <u>not</u> for the entry matrix).

Finally, multiplying two matrices together,

$$T_{half-solenoid} = \begin{bmatrix} \frac{1}{2}(1+\cos\theta) & \frac{L}{\theta}\sin\theta & \frac{1}{2}\sin\theta & \frac{L}{\theta}(1-\cos\theta) \\ -\frac{\theta}{2L}\sin\theta & \cos\theta & \frac{\theta}{2L}\cos\theta & \sin\theta \\ -\frac{1}{2}\sin\theta & \frac{L}{\theta}(\cos\theta-1) & \frac{1}{2}(1+\cos\theta) & \frac{L}{\theta}\sin\theta \\ -\frac{\theta}{2L}\cos\theta & -\sin\theta & -\frac{\theta}{2L}\sin\theta & \cos\theta \end{bmatrix}$$

This transformation is tested both symbolically and numerically. The product (exit)(½centre)(½centre)(entry) is compared with the known full-solenoid transformation. Though defined in different terms, the transformations are found equivalent.

Statistical Approach

The muon decay experiment is based on observing the same event many (~10^9) times. Consequently, it is the statistical average muon behaviour that is important to this project. The beamline x-y plane has its origin defined at the average position of muons at any z-location. Simulation should reveal spatial distributions of muons having centroids within statistical fluctuation of this origin anywhere along the beamline. Furthermore, distributions of the simulated particles should appear as "normal" populations. Failure to achieve these forms may indicate that the simulation does not consider enough particles to provide an accurate statistical representation.

Liouville's Theorem

Plotting either the x or y position with its conjugate deviation (dx or dy respectively) for a statistically significant number of particles results in a telling shape. Tracing a curve around one standard deviation of the population yields an ellipse, known as the beam ellipse. Liouville's theorem states that while the orientation of the beam ellipse may be modified, the area enclosed cannot be altered by magnetic fields. Hence, a particle source having a finite ellipse can never be "focused" down to a point.

The technique used to circumvent this thermodynamic constraint is to introduce "slits" into the beamline. Slits only pass particles with positions sufficiently close to the beam axis. Particles not passing through the slit are usually removed from the system and from consideration. However, some particles can scatter off the edges of the slits and remain in the system (further information on this phenomenon is in the latter pages of this document). If the beam ellipse is correctly tuned where the slit is positioned, the spatial filtering of particles can concurrently remove the particles with high deviation. This is the method used to reduce the overall deviation of the beam.

Experimental Method

Beamline Simulation

The design and testing of the beamline are carried out using computer simulation. In the high-energy regime, beam optics is a very reliable approximation to real behaviour even when element matrices are determined to first order. Both simulations used in this project calculate most beam-optical properties to second order. The reliability of such algorithms has been tested at TRIUMF, CERN, and other experimental locations. The first simulation calculates the aggregate transfer matrix for the beamline; the second is a Monte Carlo path tracking application. The design process is iterative – a beamline is "tuned" using the first and tested with the latter.

Intran – running the TRANSPORT algorithm

Developed at CERN, the TRANSPORT algorithm is useful for performing the matrix multiplication that is central to beam optics. The Intran application used for this project also includes some graphical capabilities and a user interface. Starting with the template muon beamline provided by TRIUMF, this code allows for the definition of degrees of freedom in the system. These adjustable parameters include element length, and magnetic field strength. By calculating the partial derivatives of the elemental transfer matrices, the adjustable parameters are iteratively set to provide a solution to an input constraint. In this project, the constraint specified relates to the aggregate transfer matrix of the system. An example input file is located in the appendix.

The Intran code is modified to allow for a half-solenoid in the beamline. The template beamline provides values for all the elements up to the half-solenoid, but the adjustable parameter set was limited to the final drift distance and the magnetic fields of the last two focusing magnets. Allowing these three degrees of freedom is sufficient to effectively set any value for the beam divergence at the target, providing of course that Liouville's theorem is not violated. Intran allows for manipulation of the transfer matrix quite easily, but the connection between the transfer matrix and statistical deviations is not provided. For this, the Revmoc simulation is used.

Revmoc – tracking individual particles

Revmoc accounts for scattering, energy loss and beam broadening, and hence provides a check for the system tuned using TRANSPORT. It requires an equivalent input file to define the beamline parameters (a sample is provided in the appendix). Additionally, a distribution of the initial beam parameters must also be supplied. Weighted by this distribution, particles are selected randomly for input to the system. Each particle is characterized by a vector of (x,y) position and conjugate momenta, as well as polarization and mass. Based on the initial conditions, the trajectory of each individual particle is followed through the beamline.

The use of apertures in Intran would be irrelevant since no scattering is taken into account. Revmoc simulates the effect of the aperture based on its size and its component material. As such, the final distribution of particles is the result of an experiment. Only a small fraction of the particles reaches the target having avoided collisions with the apertures and magnets. The target distributions are used as the data in this project to determine whether the beamline is sufficient.

Experimental Filtering

The apertures in the beamline are part of the template provided by TRIUMF. To confirm that these apertures are performing the required filtering of high-divergence particles, a Revmoc trial is carried out, and the beam ellipse is plotted at various points of interest. The graphics below are for the x-dx ellipse; similar behaviour is encountered for the y-dy ellipse.

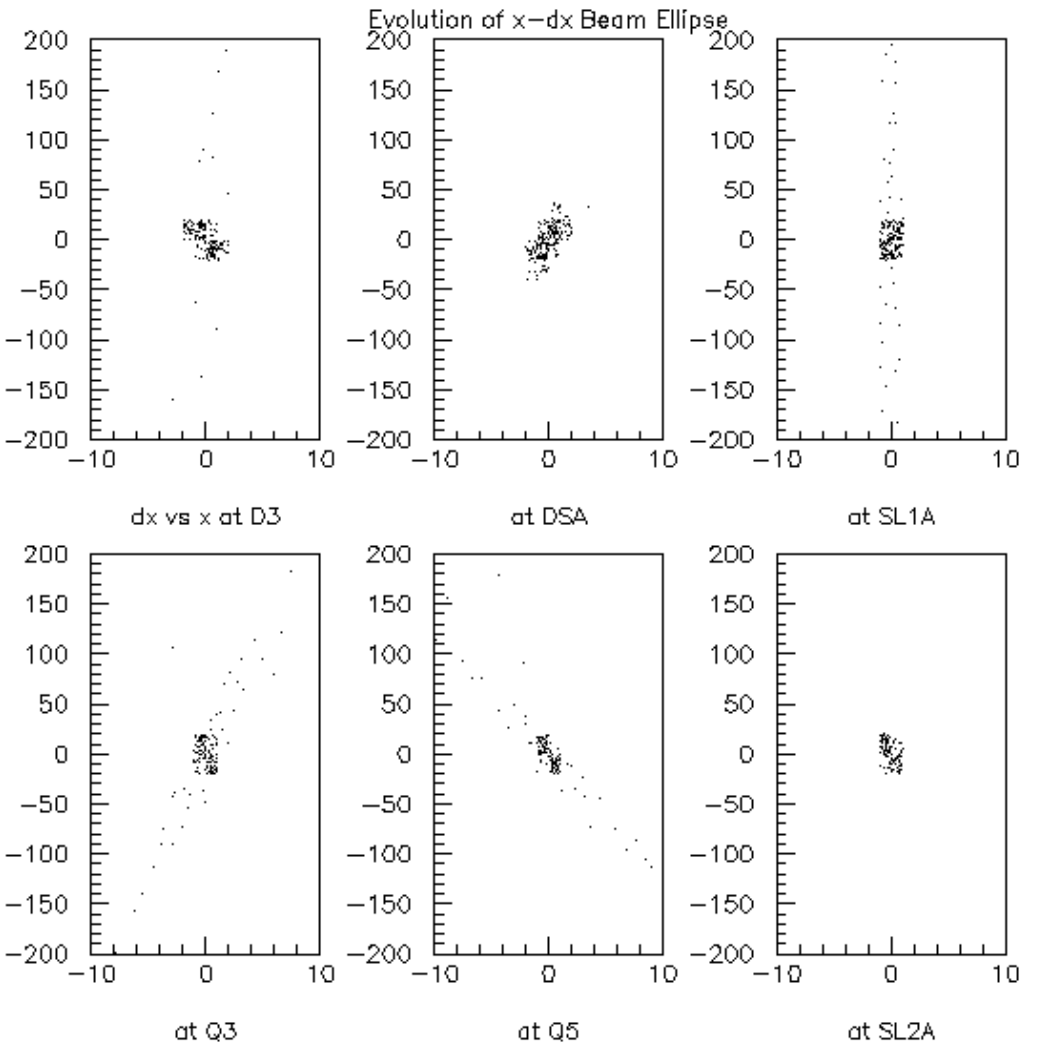

The particles pass through a small opening coming out of the source. The D3 plot is made immediately after. The scattered particles are identified by their location outside the central region of the ellipse. The drift region to DSA has the effect of rotating the previous ellipse. The SL1A plot is immediately after the first slit – the spatial filtering of the previous ellipse is apparent, as are the newly scattered particles. This new form is rotated through drift regions and the quadrupole fields of Q3 and Q5 immediately before reaching the second slit at SL2A. The plot at Q5 indicates exactly what is required – the beam ellipse is tilted ~45 degrees. Spatial filtering at this point will be most effective to reduce the beam divergence. The plot after the slit confirms that the filtering has been successful since the high divergence particles have been removed from the system.

Beamline Design

The Intran program is used to design the beamline. This simulation characterizes the beamline based exclusively on the component transfer matrices. The output is the aggregate transfer matrix at any z-position on the beamline. As a design tool, Intran allows the user to define which parameters in the system can be modified. These parameters are then adjusted to meet input constraints on the transfer matrix at a particular z-position. In all designs for this project, the constraints on the aggregate transfer matrix are defined either before the half-solenoid or at the target. Liouville's theorem has an analog as a transfer matrix limit – there are some transfer matrices that are impossible to generate with the allowed degrees of freedom. Intran will arrive at this conclusion numerically if such a impossible constraint is requested.

Based on the TRIUMF template beamline, the design is limited to three degrees of freedom for this project. This report will show that this "minimally invasive" solution is adequate to meet the beamline criteria. Preliminary design is broken down into two iterations with Intran. The first run varies the field strengths of the last two focusing magnets to obtain a desired effect without the half-solenoid in the beamline. The second run is carried out with the half-solenoid effect; it adjusts the length of the final drift region.

As a first design, the beamline is constrained to provide a "point-to-parallel" effect without the half-solenoid. This amounts to setting R22 and R44 to zero. Once the half-solenoid is added, however, the divergence increases beyond specifications. The second design imposes a "point-to-point" constraint on R21 and R43 without the half-solenoid. Once the half-solenoid is inserted and the drift region adjusted, low divergence is obtainable. The magnetic fields obtained in the second design provide the values for all following single-variable designs.

Having gained an understanding of the design concepts from these preliminary trials, several possible designs are considered in this project. The designs can be grouped into two categories. The first allows all three degrees of freedom discussed above; the second uses the magnetic fields found in the preliminary trials and only adjusts the final drift region. Zero-value constraints are applied after the half-solenoid for both categories as follows:

- R22 and R44
- R21 and R43
- R21, R22, R23, R24
- R21, R43, R23

In some cases, the elements cannot be set to zero and the design must settle for a finite value. Not surprisingly, this compromise is more pronounced in the single-variable design. All the above trials have the objective of minimizing the divergence of the beam at the target. After the preliminary trials, it became apparent that the dx (as opposed to the dy) distribution at the target was the limiting factor. The third case above attempts to address this by reducing all contributions to the final dx.

A sample output plot from Intran is shown below. In this trial, the curves show how R22 and R44 vary along the beamline. The sample plot illustrates that these zero-constraints are met at the end of the beamline.

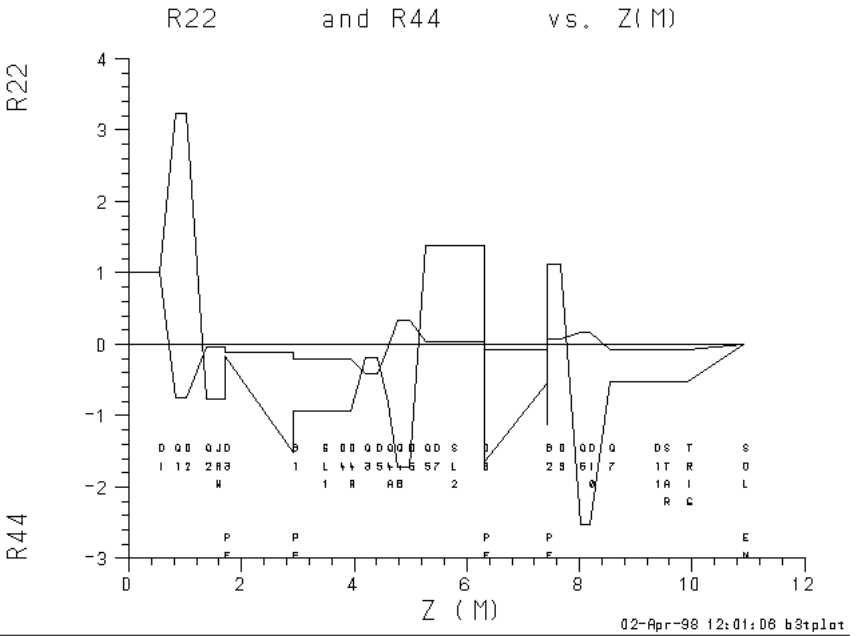

Individual particle simulation and analysis is done for each of the cases described above. In this report, the two most illustrative cases are developed in detail. These are:

- R22 and R44 with a single adjustable beamline parameter
- R21, R43 and R23 with three adjustable beamline parameters

Henceforth, these two cases will be called the single-variable and three-variable beamlines respectively.

Solenoid Facing

Interestingly, it doesn't matter to the experiment which way the half-solenoid is facing. In other words, the solenoid central field can point equivalently in the positive or negative z-direction. In the beamline upstream of the solenoid, the system is represented by a matrix that does not mix the x and y components. The upstream system, positive and negative solenoid transformations are of the form:

$$T_{sys} = \begin{bmatrix} b11 & b12 & 0 & 0 \\ b21 & b22 & 0 & 0 \\ 0 & 0 & b33 & b34 \\ 0 & 0 & b43 & b44 \end{bmatrix} \quad T_{sol+} = \begin{bmatrix} a11 & a12 & a13 & a14 \\ a21 & a22 & a23 & a24 \\ a31 & a32 & a33 & a34 \\ a41 & a42 & a43 & a44 \end{bmatrix} \quad T_{sol-} = \begin{bmatrix} a11 & a12 & -a13 & -a14 \\ a21 & a22 & -a23 & -a24 \\ -a31 & -a32 & a33 & a34 \\ -a41 & -a42 & a43 & a44 \end{bmatrix}$$

The aggregate matrices $T_{sol+}T_{sys}$ and $T_{sol-}T_{sys}$ have elements that are either identical or additive inverses. Since there is no distinction between the positive and negative x and y directions, the two possibilities have analogous effects.

Results and Analysis

The Three-Variable Beamline

With three degrees of freedom, each of R21, R43 and R23 can be set to zero. Using Revmoc to simulate one million randomly distributed particles from the source, the beam is analyzed graphically. Some interesting results are plotted below. The top two graphics show the spatial distribution of particles before and after the half-solenoid. The distributions are similar – the solenoid does not have a large spatial impact on the beam. The beam size is about 16cm horizontally and 6cm vertically. This is regrettable since a small fraction of the 3,549 particles making it to the half-solenoid will actually hit the 2x2cm target.

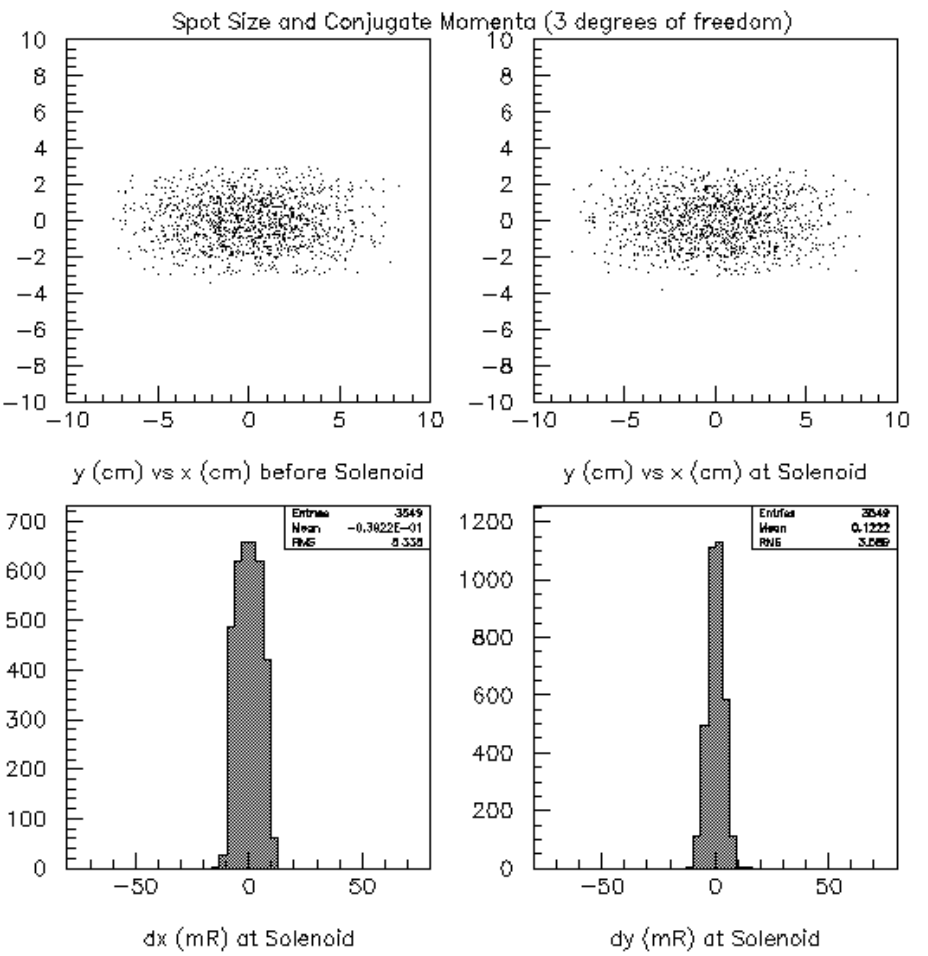

To calculate the composite divergence, the dx and dy RMS values are added in quadrature. This yields a composite divergence of 9.1mR; the requirement of 14.1mR is surpassed. The cost of this low divergence is that the efficiency suffers. This again is Liouville's theorem at work – a small divergence requires a spatially broad beam. By manipulating the three variables, any orientation of the beam ellipse can be obtained. As will be revealed in the next sections, any desirable effect can also be obtained by adjusting only the final drift region.

The Single-Variable Beamline

This section should be prefaced with the statement that the following beamline is chosen as the best. Again, Intran is used to determine the drift distance required to set the R22 and R44 entries to zero. Revmoc then tracks one million muons through the system. Compared to the previous case, the beam is spatially sharper at the target as shown below. The divergence criterion is not met by the collection of particles that pass through the half-solenoid.

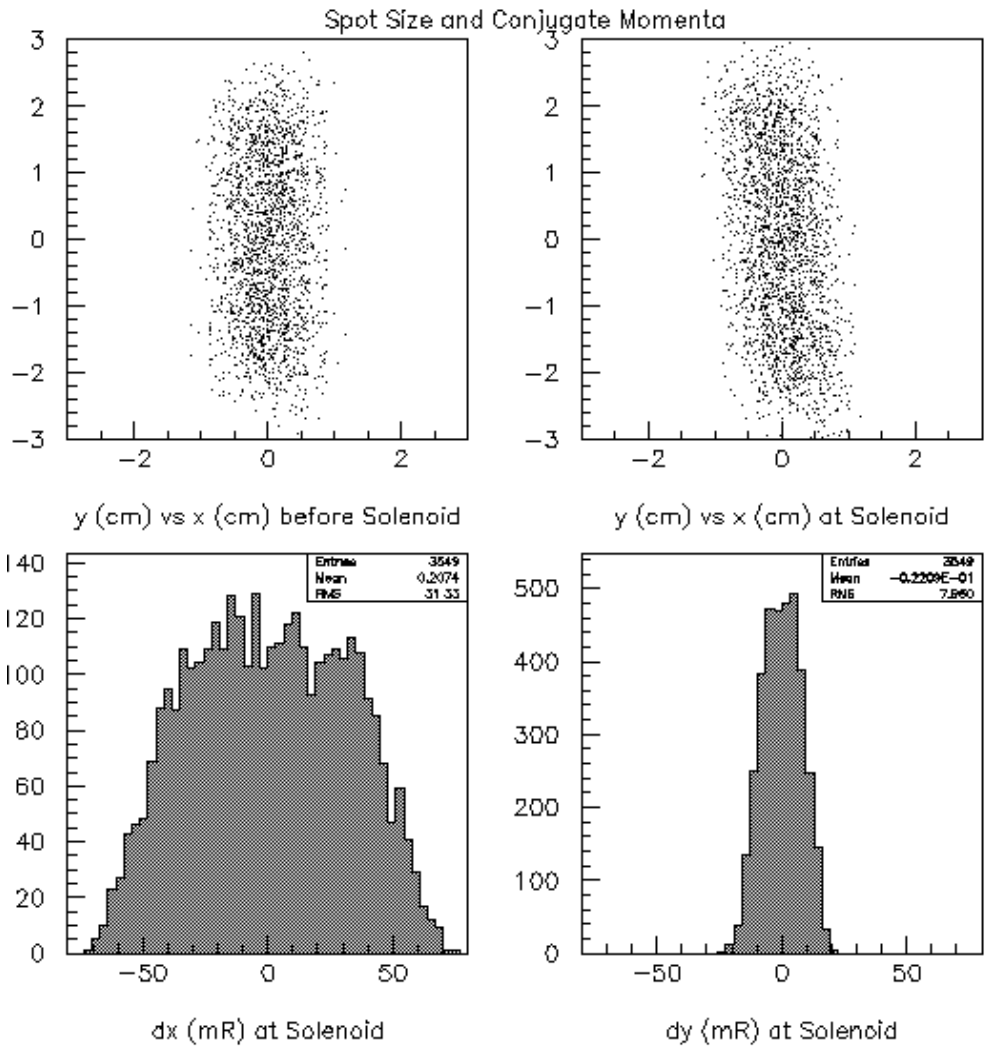

Both divergence distributions have approximately Gaussian form. This confirms that enough particles have been tracked to make the results statistically significant. Clearly, the dx distribution with an RMS value of 31.3mR causes the composite divergence to exceed 14.1mR. If, however, only the particles that are spatially located in the square target region are considered, the divergence is sufficiently small.

This effect can be appreciated by considering the beam ellipses. Actually, dx vs. y and dy vs. x are also plotted, bringing the total number of distributions to four. The spatial limits are graphically represented on the plots below with vertical lines. Any particles outside the regions enclosed by the dotted lines do not hit the 2x2cm target. The muons inside the acceptance region are defined as the selected particles.

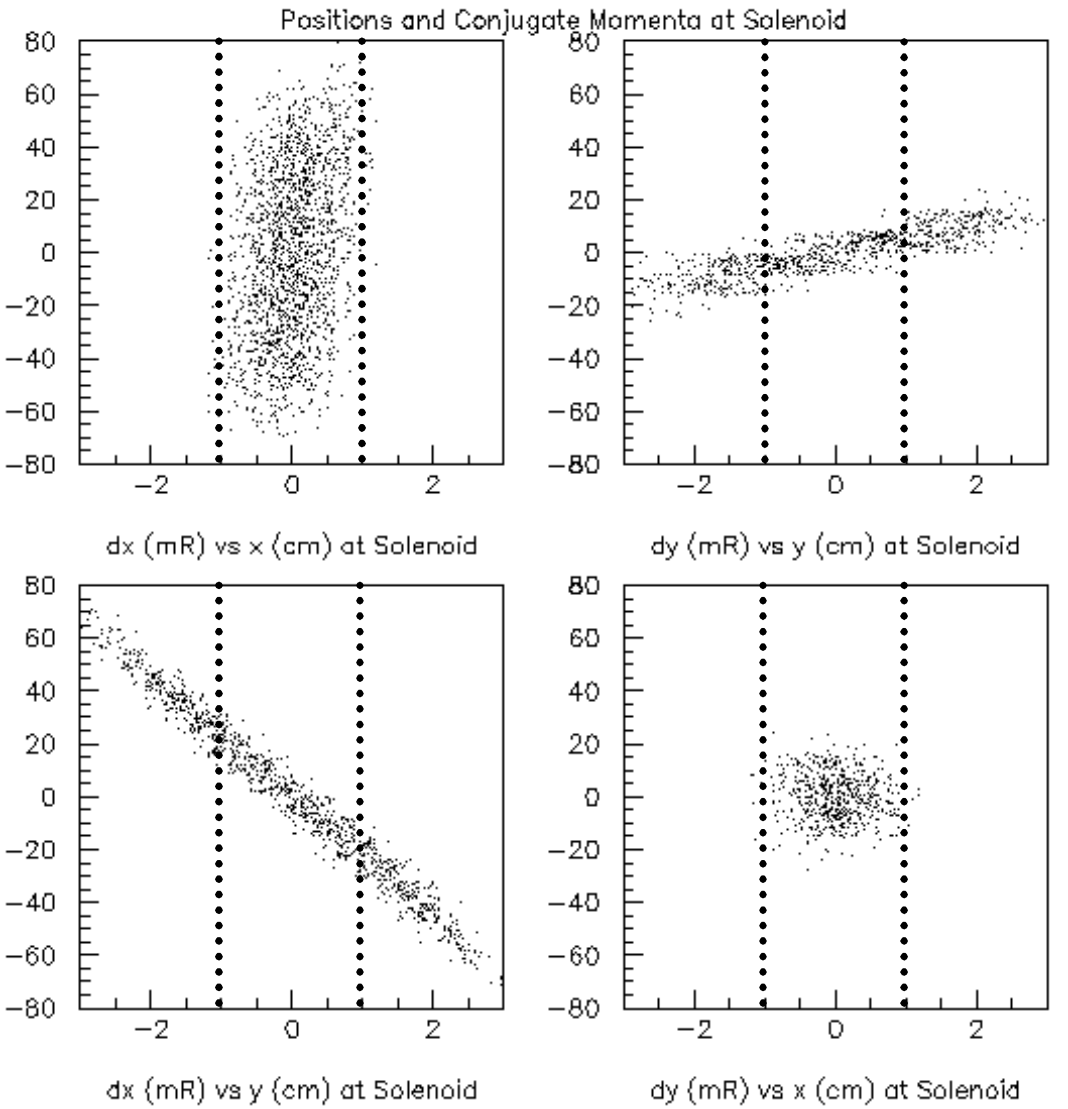

The selective shape of the target controls the beam ellipse as would an aperture. Limiting the x-position has little effect, but the y-position filtering eliminates the particles with high dx and dy values. The ~45 degree rotations of these two figures confirms that the selection is done effectively. Considering only the selected particles, the divergence distributions can be reconsidered.

Plotting only the muons that lie within the selection regions, the distributions are:

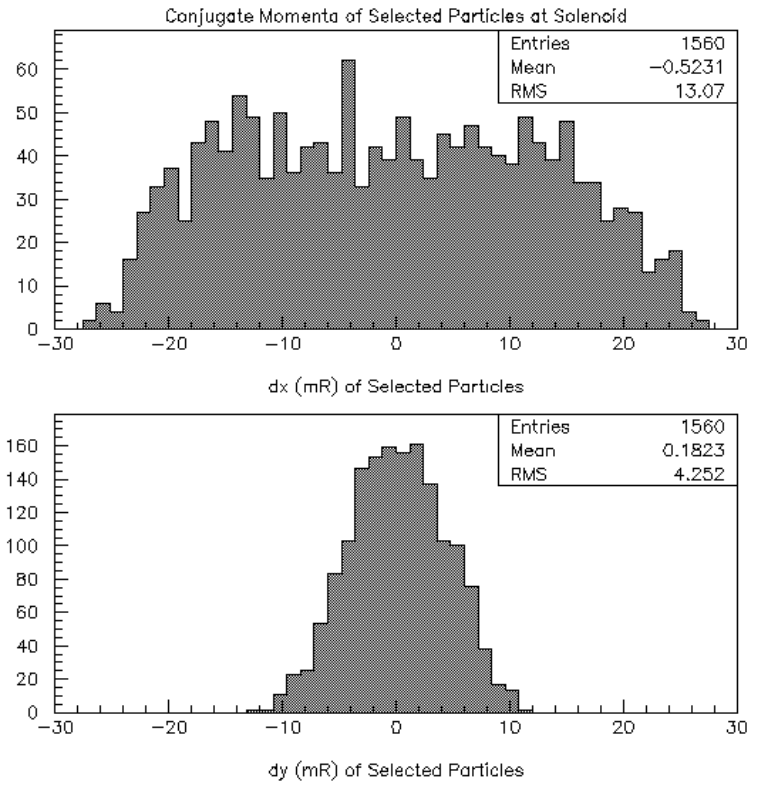

The divergence in both dx and dy is considerably smaller. The composite divergence is 13.9mR, which just meets the divergence requirement - this is arguably the optimal value. There is still a 0.2mR allowance for statistical fluctuation and uncertainty in the elemental fields, yet the value is close enough to 14.1mR to keep the efficiency as high as possible. The number of selected muons is 1560 in this trial, giving an efficiency of 1560/1,000,000 = 0.156%. This is typical of beamline designs.

Scattering in the Beamline

When muons scatter, their spin-polarization changes unpredictably. In the worst case, a scattered muon reaching the target could have a polarization completely opposite to the desired direction. Comparing this to the errors caused by divergence, this would be equivalent to a particle with 3,142mR divergence! Because of this, the scattering must be kept to a minimum in the system.

In addition to losing polarization, scattered muons also lose momentum. Hence, by engineering the beamline to select only the muons with the highest possible momentum, the scattered muons will be removed from the system. Results obtained by Dr. Nathan Rodning [4] indicate the correlation between lost polarization and momentum. In addition to providing a selection mechanism, this phenomena also suggests a method for determining which particles have scattered in a simulation – simply look for those with reduced momentum.

The results below show the momentum of the muons along the single-variable beamline. Only 100,000 particles are simulated because data is collected at the source. This requires writing information for all particles considered and quickly exhausts available memory on the computer.

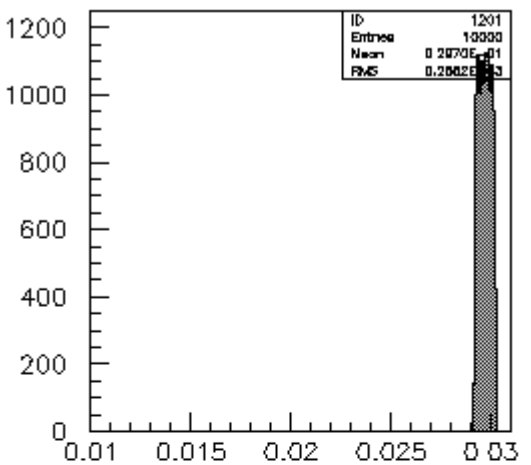

Initial Momentum Distribution

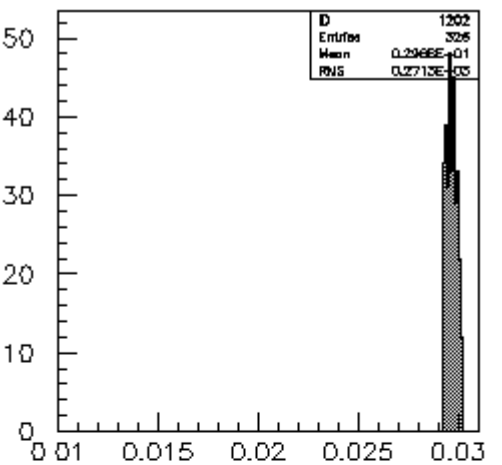

Momentum Distribution after Jaws

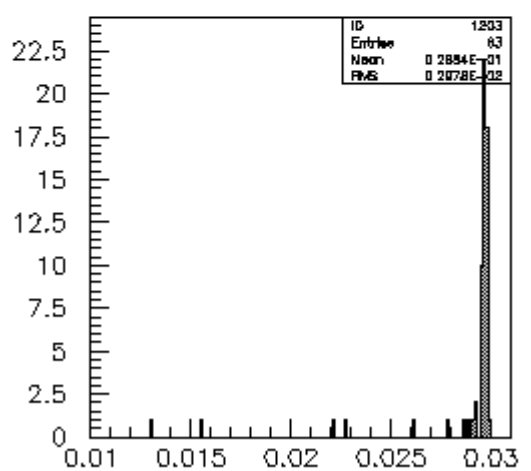

Momentum Distribution after Slits (D4)

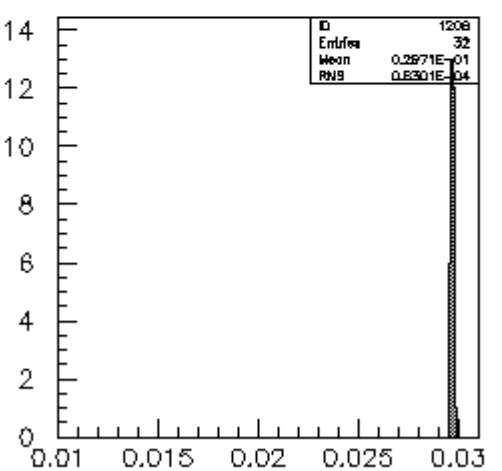

Momentum Distribution after Solenoid

As anticipated, scattering is observed following the slits – the scattered particles have less momentum. When the particles reach the solenoid, the scattered particles are no longer in the beamline. The final bending magnet separates the scattered particles from the beamline. A final slit cannot be placed at the entrance to the solenoid, as the scattered particles would reach the target. The momentum distribution at the target is sharp having selected only a fraction of the initial muons from the source. These plots also show how the number of muons in the system decreases as they travel away from the source. The majority of muons are lost coming out of the source at the “Jaws” of the emitter. The efficiency of ~0.3% from source to the half-solenoid (including those not spatially selected by the target) matches the previous results for this beamline design.

The experiment with one million particles discussed earlier (data only being recorded at the end of the solenoid) reveals similar results – no scattered muons reach the target. Still, this represents only 3540 events at the target and cannot definitely ensure that fewer than one in ten thousand muons at the target will have been scattered. Such a computation would require at least 100,000,000 particles to be statistically significant – this computation is prohibitive due to CPU and memory constraints. This is the nature of many phenomena in beamline simulation. However, it is reassuring that even for the small number of events examined here, scattered particles are removed from the system. Had scattered particles not been observed at any point in the beamline, the results would not be as concrete.

Sensitivity to Initial Beam Parameters

The initial divergence and size of the beam is provided in data from TRIUMF. However, the project should be immune to small fluctuations in these initial parameters. The case where the initial divergence and size of the beam are sharper than specified is not worth considering – this gives rise to a smaller beam ellipse and is consequently less demanding. To endure that the design is robust with respect to the initial parameters, the following changes are made:

- Initial x: 0.85cm→1.0cm
- Initial y: 0.50cm→1.0cm
- Initial dx: 130mR→400mR
- Initial dy: 330mR→400mR

These changes increase the beam size and average divergence by around two times. Source fluctuations should be nowhere near these limits.

Even with this increase, the divergence criterion is still met. With one million events, however, the overall efficiency of selected particles drops to 0.0027%! Hence the beam should be made as parallel as possible at the source to increase the overall efficiency of the system. However, controlling the initial conditions may limit the number of particles produced at the source.

Sensitivity to Solenoidal Field

The detection solenoid is nominally 2m long with a central field of 2T. The target is placed at 1m into the solenoid. The possibility that the target location is inexact is not considered. The possibility that the field is wrong should be examined. It may be that the field truly is 2T, but the solenoid transfer matrix is inevitably not an exact representation of the physical object. Hence, the beamline is simulated with a modified solenoidal field. In addition to numeric increases and decreases in the central field strength, the entry field is scaled as well. These two modifications are carried out independently.

The central field is varied from 1T to 3T; the entry field is scaled from ½ to twice its original strength. For modifications within $\pm$5% in either the central or the fringe field, the divergence requirement is still met. Additionally, scatted particles do not reach the target for any of the trials. Outside the 5% error margin, the beam's composite divergence at the target exceeds the 14.1mR limit. In this case, the beam can be made suitable by readjusting the length of the final drift region. Should this situation arise, an analysis similar to that presented in this report would be required to confirm the suitability of the beamline.

Final Drift Region Distance

The distance between the final quadrupole magnet and the solenoid entrance is a parameter that can be experimentally set precisely. Hence, the modification of this distance in simulations is not done to test error boundaries, but rather in hopes of confirming that this drift distance is optimal. Simulations were done with 100,000 particles starting from the source, varying the final drift distance by $\pm$0.4, and $\pm$0.2, as well as the control case (the single-variable beamline discussed previously). Distributions for x and y are plotted at the target, their RMS values recorded. Particles hitting the target in the [-1 1] spatial square are selected and their divergence plotted. The following graph is a summary of the results.

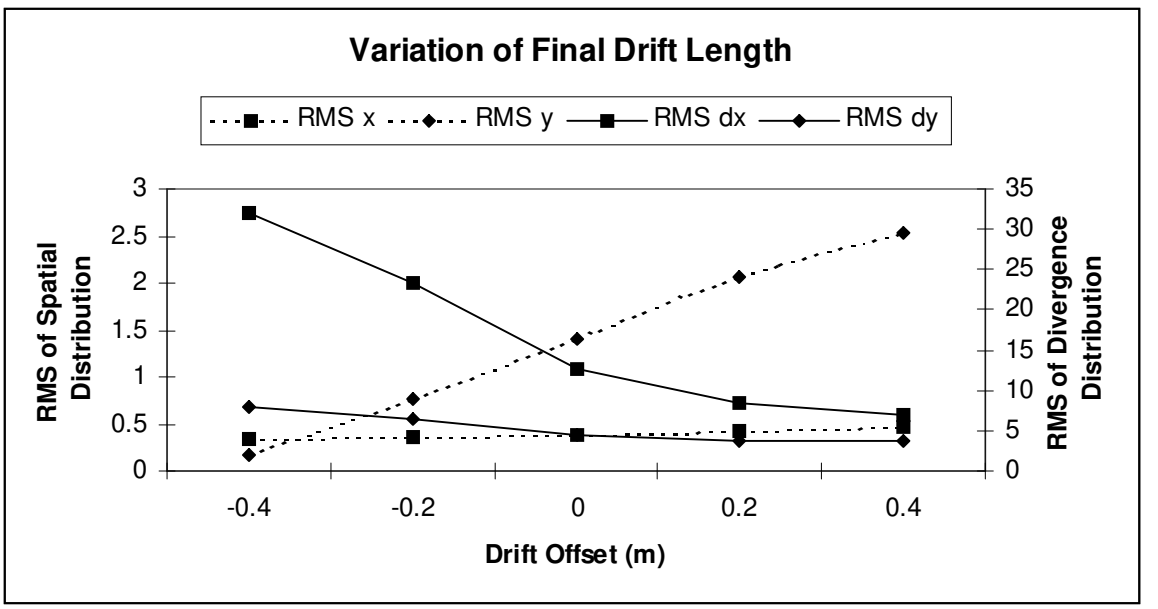

Many observations can be made from the above plot concerning the distance range of –0.4m to 0.4m. All curves are monotonic in this region suggesting that interpolation is prudent. The y-distribution in particular becomes much wider as the drift region is lengthened resulting in more particles falling outside the square target. By design, these particles also have the high dx and dy and the divergence distribution of the selected particles becomes accordingly sharper. Both the dx and dy RMS values are decreased when as the drift offset increases. This is a clear example of how spatial filtering works with Liouville's theorem. The price of the smaller divergence is apparent from the following table.

Drift Offset (m)	Composite Divergence (mR)	Number of Particles Hitting Target
-0.4	32.9	315
-0.2	24.1	244
0	13.3	142
0.2	9.2	99
0.4	7.8	78

The control case shows a smaller divergence than previously obtained (13.9mR). This is not cause for concern. This trial tracks $1/10^{th}$ of the particles of the earlier trial, and hence 13.9mR is more valid statistically. Increasing the drift length has two effects:

- the divergence of the selected particles decreases
- the number of selected particles decreases

This is a now-familiar trade-off. To satisfy all beamline criteria, the beam with divergence just below 14.1mR should be selected as this provides the necessary precision with the highest possible number of events. The fact that this selects the control case supports the selection of this beam parameter in the first place. Additionally, this test shows that the divergence of the beam at the target can be varied significantly (along with the efficiency) simply by manipulating the length of the final drift region.

Conclusions

For an experiment to measure the Michel parameters of muon decay, a beam of spin-polarized positive muons is required. The spin-polarization is key to the precise nature of the experiment. A muon source is available that emits initially spin-polarized muons. The function of a beamline must be to preserve this by reducing scattering in the system as well as limiting the polarized muons to a small divergence at the detecting target. Specifically, fewer than one in ten thousand muons may scatter and still reach the target; the RMS divergence of the beam at the target must have a value not more than 14.1mR. This report outlined the successful design of several muon beams meeting these requirements. The selected beamline is the one with the highest efficiency – the highest proportion of muons reaching the target.

The system is initially designed by simulating the detecting half-solenoid at the end of the TRIUMF muon beamline. The beam-optical effect of the half-solenoid is derived and its effects programmed into the simulation software. Simply by varying the distance between the final focusing magnets and the solenoid, the divergence of the beam can be set to the required value. The drift region length of the chosen beamline is 1.32346m. The computational simulation of this beamline provides an overall efficiency of 0.156% and a combined divergence of 13.9mR at the target. Of the 1560 particles reaching the target, none had scattered.

The design is robust with respect to the initial beam parameters. An exaggerated simulation of the degradation of the quality of the source sustains the divergence and scattering requirements. However, the efficiency of the beamline drops considerably when the initial beam parameters are worsened. This suggests that the initial distribution of muons should be kept as parallel as possible.

The sensitivity of the design with respect to the solenoidal fields is greater. Changing either the fringe or the central field by more than $\pm$5% leads to excessive divergence at the target. If the field of the solenoid is outside of this error boundary from its nominal value, the beamline may need redesigning. Once the solenoid is physically set-up for the experiment, its field may differ from the predicted value. It is speculated that the beamline can be rendered suitable with the adjustment of a single parameter: the final drift length.

The size of the target is an asset to the selection of suitable muons. The effect of the target size and shape on the measurement of the Michel parameters is outside the scope of this project, but the target could be tailored to provide the highest efficiency for a given divergence requirement. Such a design could be accomplished by selecting muons enclosed within an arbitrary spatial area as determined by the simulation. The divergence of the particles selected by the target could then be plotted in much the same manner as it is done in this report.

The biggest constraint on the validity of the results is the quantification of muon scattering. With 1560 events, it is not possible to ascertain undoubtedly that there is less than 10^{-4} probability that a selected particle has been scattered. The limiting factor in further pursuing this question is computational power. The fact that many scattered particles were observed in the beamline is reassuring in that all were removed before reaching the target.

References

1. Carey, D. The Optics Of Charged Particle Beams. Harwood Academic Publishers (1987).

2. Engfer, R., Walter, H. K. Ann. Rev. Nucl. Part. Sci. 36: 327 (1986).

3. Gill, D. R. TRIUMF E614 NSERC grant proposal

4. Rodning, N. U of A Colloquium presentation (1997)

5. Stinson, G.M. U of A Physics 555 Course Notes (1991)

6. INTRAN – A user friendly interface to TRANSPORT

7. REVMOC – A Monte Carlo beam transport program

Appendix A – Sample Intran Input File

The following text is an input file for Intran to fit the beamline to the R22 = R44 = 0 constraint at the target. Each entry represents one magnetic element and hence one transfer matrix. Of particular interest are the final five entries:

- D11 is the drift length variable which is adjustable in this fit – initialized to 1m
- SOL is a 2m solenoid with a 20kGauss central field and the target at 0.5 length
- FIT1 sets R22 at this location to 0, within 0.001
- FIT2 sets R44 at this location to 0, within 0.001
- END marks the end of the beamline

```
'M13 BEAMLINE WITH HALF SOLENOID 98/02/25 FITTING R22 AND R44 ELEMENTS AT TARGET'
    0
   1.000000       '    '      0.42000    65.00000     0.25000   165.00000
                               0.00000     0.50000     0.02970;
   3.0            'D1  '      0.54150;
   5.00           'Q1  '      0.29300    -1.00556    10.31900;
   3.0            'D2  '      0.17687;
   5.00           'Q2  '      0.36322     0.82695    15.55750;
   3.0            'JAW '      0.18110;
   3.0            'D3  '      0.16120;
  16.00           '    '      5.00000    10.00000;
  16.00           '    '      7.00000     0.50000;
  16.00           '    '      8.00000     4.40000;
   2.0            'PF11'     20.00000;
   4.000          'B1  '      1.21080     0.85685     0.00000;
   2.0            'PF12'     40.00000;
   3.0            'SL1 '      0.52700;
   3.0            'D4  '      0.31000;
   3.0            'D4A '      0.16680;
   5.00           'Q3  '      0.27432     1.07707    10.16000;
   3.0            'D5  '      0.21220;
   5.00           'Q4A '      0.18161    -1.37503    15.55750;
   5.00           'Q4B '      0.18161    -1.37503    15.55750;
   3.0            'D6  '      0.21220;
   5.00           'Q5  '      0.27432     0.99810    10.16000;
   3.0            'D7  '      0.16680;
   3.0            'SL2 '      0.31000;
   3.0            'D8  '      0.56000;
  20.0            '    '    180.00000;
   2.0            'PF21'     40.00000;
   4.000          'B2  '      1.12155     0.92488     0.00000;
   2.0            'PF22'     20.00000;
  20.0            '    '    180.00000;
   3.0            'D9  '      0.22940;
   5.00           'Q6  '      0.36322     0.80216    15.55750;
   3.0            'D10 '      0.16778;
   5.00           'Q7  '      0.36322    -0.89988    15.55750;
   3.1            'D11 '      1.00000;
   19.0           'SOL'       2.00000    20.00000     0.50000;
   10.            'FIT1'     -2.00000     2.00000     0.00000     0.001 ;
   10.            'FIT2'     -4.00000     4.00000     0.00000     0.001 ;
   3.             'END'       0.00001;
 SENTINEL
 SENTINEL
```

Appendix B – Sample Revmoc Input File

This file represents the beamline adjusted by Intran from the input in Appendix A. Apertures and initial beam conditions are now entered. Some of the labels change, but the two definitions are equivalent. In particular, the previous D11 is now D12 that assumes the length fit by Intran. The entries with a "*" marker are apertures.

```
0 Fit by Intran file "m13_2244"
T TARG .01  .1  0.  0.  0.  135.0  ! 1.0 cm thick target, 10 cm wide, 135 deg
D D1 0.24 15.
D SL0 .001 15.
D  0.3005 15.
QUAD Q1 .293  -1.00556 10.319
D D2 .17687  15.
QUAD Q2 .36322  .82695 15.5575
D DJ .1801  15.
D JAWS * .001  10.0 0.0025 8.96 1.5  -1.5  1.5  -1.5 0.0 0.0 1.0 29.0
D D3 .1612  15.
ENTR  20.0                          ! dipole pole face inclined at 20 degrees
BEND  1.2108  .85685  0.0  0.0  .0297
EXIT 40.0                           ! dipole pole face inclined at 40 degrees
D DSA .126 20.0
D .041 15.
D * .01  10.0 .0025 8.96 0.55  -0.55  5.05  -5.05 0.0 0.0 1.0 29.0
D SL1A  * .10  10.0 .0025 8.96 0.50  -0.50  5.  -5. 0.0 0.0 1.0 29.0
D D4 * 0.7268 10. .0025 8.96 0.50  -0.50  5.  -5. 0.0 0.0 1.0 29.0
QUAD Q3 .27432  1.07707  10.16
D D6 .2122  10.
QUAD Q4A .18161  -1.375  15.5575
QUAD Q4B .18161  -1.375  15.5575
D D7 .2122  10.
QUAD Q5 .27432  0.9981 10.16
D D8  .1668  10.
D DSC .019 10.0
D .041 15.
D * .01  10.0 .0025 8.96 0.55  -0.55  5.05  -5.05 0.0 0.0 1.0 29.0
D SL2A  * .1  10.0 .0025 8.96 0.50  -0.50  5.  -5. 0.0 0.0 1.0 29.0
D DSD .14 10.0
D D9 .56 10.
ROTATE 180.0
ENTR  40.0
BEND  1.12155  .92488  0.0 0.0 .0297
EXIT  20.0
ROTATE -180.0
D D10 .2294  15.
QUAD Q6 .36322  .80216 15.5575
D D11 .16778  15.
QUAD Q7 .36322  -.89988 15.5575
D D12 1.32346 15.
SOLE SOL1 1.0 -20.0 1.0 0.000001 ! kill exit field setting to small (nonzero) #
D T1 0.0001 15.                  ! Target actually inside solenoid
XSIZE  .84  130.0          ! 1.01 cm wide beam, 40 mR divergence
YSIZE  .5  330.0         ! 1.01 cm wide beam, 190 mR divergence
P .0297 .001 .0297 .0001     ! 0.0297 GeV/c , fw=0.001GeV/c, mom axis, en thresh
MASS  .105659  0.  0.  0. 0. 1.0
INIT SEED 11110
GROUP  1.  1000.000  0.  0.  0.  0.  ! 1,000,000 events
OUTPUT 2.  SOL1 D12             ! output at 2 positions, labeled as listed
END
FINI
```

Appendix C – Sample Revmoc Output

The following is a sample of the data recorded by Revmoc. Each section represents one particle at a particular beamline location in this order:

- x position [cm]
- dx divergence [mR]
- y position [cm]
- dy divergence [mR]
- momentum [GeV/c]
- mass
- weight 1 (not used)
- weight 2 (not used)
- z coordinate [m]
- time (not used)
- polarization – 1 indicates spin-polarization opposite to momentum
- particle identification number
- beamline position – label corresponding to this z coordinate

```
    0.254  -0.145E+01   1.071   0.251E+02 0.02967   0.105659  0.100E+01  0.100E+01
   9.8732  0.1218E-06   1.0000     382 D12

    0.149  -0.248E+02   1.187   0.382E+01 0.02967   0.105659  0.100E+01  0.100E+01
10.8732  0.1218E-06   1.0000     382 SOL1

   -0.067  -0.259E+01  -1.295  -0.377E+02 0.02974   0.105659  0.100E+01  0.100E+01
9.8732  0.1216E-06   1.0000     445 D12

    0.060   0.358E+02  -1.485  -0.121E+02 0.02974   0.105659  0.100E+01  0.100E+01
10.8732  0.1216E-06   1.0000     445 SOL1

   -0.548  -0.378E+01  -0.106   0.129E+01 0.02976   0.105659  0.100E+01  0.100E+01
9.8732  0.1215E-06   1.0000     806 D12

   -0.571  -0.226E+01  -0.113  -0.330E+01 0.02976   0.105659  0.100E+01  0.100E+01
10.8732  0.1215E-06   1.0000     806 SOL1

    0.098  -0.179E+01  -0.091  -0.772E+01 0.02962   0.105659  0.100E+01  0.100E+01
9.8732  0.1220E-06   1.0000    1848 D12
```

Appendix D – Sample Paw Macro File

This macro, executed in a visualization program called Paw, reads in the Revmoc output and generates the nice graphics found throughout this report.

```
ntupl/create 100 m13 12 ' ' 1000 x dx y dy p m w wd z t pol number
ntuple/read 100 m13_2.dat ' '  ' ' 100000
ntuple/cuts $1 z<10.0
ntuple/cuts $2 z=9.9497
ntuple/cuts $3 z>10.0
ntuple/cuts $5 x>-1.0.and.x<1.0.and.y>-1.0.and.y<1.0
histo/create/2d 2301 'dx (mR) vs x (cm) at Solenoid' 20 -5.0 5.0 20 -30.0 30.0
histo/create/2d 2302 'dy (mR) vs y (cm) at Solenoid' 20 -5.0 5.0 20 -30.0 30.0
histo/create/2d 2303 'dx (mR) vs y (cm) at Solenoid' 20 -5.0 5.0 20 -30.0 30.0
histo/create/2d 2304 'dy (mR) vs x (cm) at Solenoid' 20 -5.0 5.0 20 -30.0 30.0
histo/create/1d 1101 'dx (mR) at Solenoid' 50 -80.0 80.0
histo/create/1d 1102 'dx (mR) before Solenoid' 50 -150.0 150.0
histo/create/1d 1103 'x (cm) at Solenoid' 50 -5.0 5.0
histo/create/1d 1104 'x (cm) before Solenoid' 50 -5.0 5.0
histo/create/1d 1105 'dy (mR) at Solenoid' 50 -80.0 80.0
histo/create/1d 1106 'y (cm) at Solenoid' 50 -5.0 5.0
histo/create/1d 1107 'dy (mR) before Solenoid' 50 -150.0 150
histo/create/1d 1108 'p at Solenoid' 1000 0 1000
hi/cr/2d 2201 'y (cm) vs x (cm) at Solenoid' 20 -3.0 3.0 20 -3.0 3.0
hi/cr/2d 2202 'dx (mR) vs x (cm) at Solenoid' 20 -3.0 3.0 20 -80.0 80.0
ntuple/project 2201 100.y%x uwfunc=$3
ntuple/project 2202 100.dx%x uwfunc=$3
ntuple/project 2301 100.dx%x uwfunc=$3
ntuple/project 2302 100.dy%y uwfunc=$3
ntuple/project 2303 100.dx%y uwfunc=$3
ntuple/project 2304 100.dy%x uwfunc=$3
ntuple/project 1101 100.dx uwfunc=$3
ntuple/project 1102 100.dx uwfunc=$1
ntuple/project 1103 100.x uwfunc=$3
ntuple/project 1104 100.x uwfunc=$1
ntuple/project 1105 100.dy uwfunc=$3
ntuple/project 1106 100.y uwfunc=$3
ntuple/project 1107 100.dy uwfunc=$1
ntuple/project 1108 100.p uwfunc=$3
zone 2 2
set htyp 1
opt -n stat
hi/pl 2201
hi/pl 2202
opt stat
hi/pl 1101
hi/pl 1105
```